International Journal of Aerospace Sciences 2013, 2(1): 16-28
DOI: 10.5923/j.aerospace.20130201.03

Static Analysis of Laminated Piezoelectric Cylindrical Panels

J. E. Jam[1,*], S. Maleki[2], A. Andakhshideh[2]

[1]Composite Materials and Technology Center, MUT, Tehran, Iran
[2]Department of Mechanical Engineering, Faculty of Engineering, Ferdowsi University of Mashhad, Mashhad, Iran

Abstract The Static analysis of laminated piezoelectric cylindrical shells with various boundary conditions is presented employing Generalized Differential Quadrature (GDQ) method. The first-order shear deformation theory (FSDT) is considered to model the static response of panel. Different symmetric and asymmetric lamination sequences together with various combinations of clamped, simply supported and free boundary conditions are considered. Particular interest of this study regards to asymmetric piezoelectric orthotropic cylindrical panels having free edges and subjected to general electromechanical loading. Taking into account the effects of shear deformation and initial curvature, a system of fifteen first order partial differential equations (PDEs) in terms of unknown displacements, rotations, moments and forces is developed. Several numerical examples are presented to demonstrate the accuracy and convergence of the proposed method with relatively small number of grid points. It is also revealed that the present method offers similar order of accuracy for all variables including displacements and stress resultants. Further results for panels with particular boundary conditions are provided which can be used as benchmarks in future.

Keywords Static Analysis, Piezoelectric Cylindrical Panel, Asymmetric Cross-ply Laminates, Generalized Differential Quadrature, Various Boundary Conditions

1. Introduction

Laminated Piezoelectric structures have found wide applications as key structural elements due to enhanced electro-mechanical characteristics[1-7]. In particular, bending, buckling and vibration of laminated piezoelectric cylindrical panels subjected to various combinations of loading and boundary conditions have been the main subject of many investigations[8-15]. It is well-known that analytical methods are only applicable to particular types of boundary conditions such as panels with at least two opposite sides simply supported. In this regard, Chen et al.[16] presented an exact elasticity solution for an orthotropic cylindrical shell with piezoelectric layers. Kapuria *et al.*[17] demonstrated similar study to obtain an analytical solution for free vibration of simply supported piezoelectric laminated circular panels in cylindrical bending. They employed a layerwise expanding in Fourier series together with the modified Frobenius method. Daneshmehr *et al.*[18] investigated dynamic response of cross-ply laminated panels with a piezoelectric layer. They found a three-dimensional elasticity solution for finitely long, simply-supported shell panels. In this paper the highly coupled partial differential equations reduced to ordinary differential equations with variable coefficients by means of trigonometric function expansion in circumferential and longitudinal directions. This method also applied to functionally graded piezoelectric (FGP) cylindrical shell panels under pressure and electrostatic excitation, recently [19]. So, in the range of analytical solutions one can find similar studies for laminated piezoelectric cylindrical panels and shell, while they are all limited to special cases of geometries, simplified theories and boundary conditions. Thus, numerical techniques, as alternatives to analytical approaches, have been developed to obtain solutions for different structural components subjected to various types of loading and boundary conditions. Among these numerical studies, one can refer to boundary element[20], dynamic relaxation[21], extended Kantorovich method[22], various meshless methods[23], differential quadrature method (DQ)[24-25], differential cubature method (DC)[26], and generalized differential quadrature (GDQ)[27].

In this paper, the GDQ method is employed to obtain a solution for static analysis of laminated cylindrical panel with piezoelectric layers. General laminate layups and any combination of various boundary conditions are considered. Accuracy and rapid convergence of the method are examined with various examples. Of particular interests in this study are panels with free edges under electromechanical loading, whereas similar results are not found in the open literature to the best of authors' knowledge. Predictions of the presented

* Corresponding author:
jejam@mail.com (J. E. Jam)
Published online at http://journal.sapub.org/aerospace

method for various stress and displacement components exhibit a good agreement compared with other solutions.

2. Governing Equations

Consider a piezoelectric laminated cylindrical panel with length a, mean radius R, total angle α and total thickness h as shown in Figure 1. The curvilinear coordinate system is located on the mid-surface of the laminate. The coordinates in the longitudinal, tangential and radial directions are designated by x, θ, *and* z, respectively and are depicted in Figure 1. According to the first order shear deformation theory, the displacement field can be written as:

$$\begin{aligned} u &= u_0(x,\theta) + z\,\beta_x(x,\theta), \\ v &= v_0(x,\theta) + z\,\beta_\theta(x,\theta) \\ w &= w_0(x,\theta) \end{aligned} \tag{1}$$

where u_0, v_0 and w_0 denote the displacements of the middle surface, β_x and β_θ are the rotation of tangents to the middle surface. Strain-displacement relations for a cylindrical shell in terms of cylindrical coordinates can be expressed as:

$$\begin{Bmatrix} \varepsilon_x \\ \varepsilon_\theta \\ \gamma_{x\theta} \\ \gamma_{xz} \\ \gamma_{\theta z} \end{Bmatrix} = \begin{bmatrix} 1 & 0 & 0 & 0 & 0 & 0 \\ 0 & \dfrac{1}{(1+z/R)} & 0 & 0 & 0 & 0 \\ 0 & 0 & 1 & \dfrac{1}{(1+z/R)} & 0 & 0 \\ 0 & 0 & 0 & 0 & 1 & 0 \\ 0 & 0 & 0 & 0 & 0 & \dfrac{1}{(1+z/R)} \end{bmatrix} \times \left[\begin{Bmatrix} \varepsilon_x^0 \\ \varepsilon_\theta^0 \\ \gamma_x^0 \\ \gamma_\theta^0 \\ \mu_x^0 \\ \mu_\theta^0 \end{Bmatrix} + z \begin{Bmatrix} \kappa_x \\ \kappa_\theta \\ \eta_x \\ \eta_\theta \\ 0 \\ 0 \end{Bmatrix} \right] \tag{2}$$

where

$$\begin{aligned} &\varepsilon_x^0 = u_{0,x}; \quad \varepsilon_\theta^0 = R^{-1}(v_{0,\theta} + w_0); \quad \gamma_x^0 = v_{0,x}; \quad \gamma_\theta^0 = R^{-1}u_{0,\theta}; \quad \kappa_x = \beta_{x,x} \\ &\kappa_\theta = R^{-1}\beta_{\theta,\theta}; \quad \eta_x = \beta_{\theta,x}; \quad \eta_\theta = R^{-1}\beta_{x,\theta}; \quad \mu_x^0 = w_{0,x} + \beta_x; \quad \mu_\theta^0 = R^{-1}(w_{0,\theta} - v_0) + \beta_\theta \end{aligned} \tag{3}$$

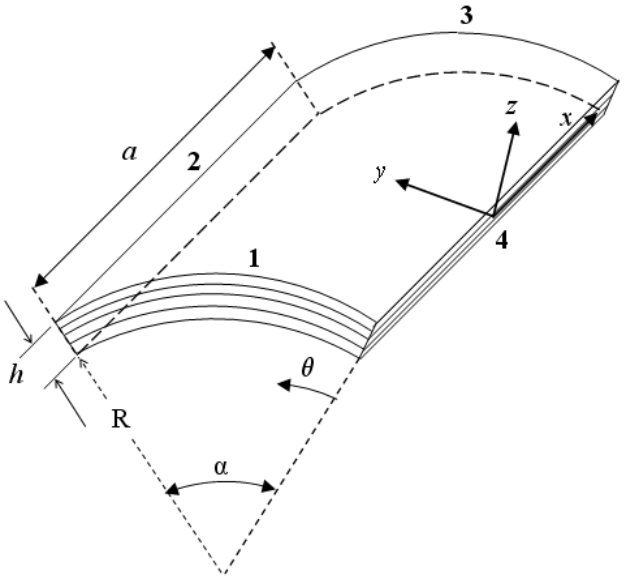

Figure 1. Geometry of the panel

In the above equations, $\varepsilon_x{}^0$ and $\varepsilon_\theta{}^0$ are the normal strains, $\gamma_x{}^0$ and $\gamma_\theta{}^0$ are the in-plane shear strains, κ_x and κ_θ are the change in the curvature, η_x and η_θ denote the torsion, $\mu_x{}^0$ and $\mu_\theta{}^0$ are the shear strains of the referenced mid-surface. Subscript comma denotes the differentiation with respect to x or θ.

The stress-strain relations for the k^{th} layer of the general laminated piezoelectric cylindrical panel in the laminate coordinate system can be expressed as follows[28-29],

$$\begin{Bmatrix}\sigma_x\\ \sigma_\theta\\ \tau_{\theta z}\\ \tau_{xz}\\ \tau_{x\theta}\end{Bmatrix}_k = \begin{bmatrix}\bar{Q}_{11} & \bar{Q}_{12} & 0 & 0 & \bar{Q}_{16}\\ \bar{Q}_{12} & \bar{Q}_{22} & 0 & 0 & \bar{Q}_{26}\\ 0 & 0 & \bar{Q}_{44} & \bar{Q}_{45} & 0\\ 0 & 0 & \bar{Q}_{45} & \bar{Q}_{55} & 0\\ \bar{Q}_{16} & \bar{Q}_{26} & 0 & 0 & \bar{Q}_{66}\end{bmatrix}_k \begin{Bmatrix}\varepsilon_x\\ \varepsilon_\theta\\ \gamma_{\theta z}\\ \gamma_{xz}\\ \gamma_{x\theta}\end{Bmatrix}_k - \begin{bmatrix}0 & 0 & \bar{e}_{31}\\ 0 & 0 & \bar{e}_{32}\\ \bar{e}_{14} & \bar{e}_{14} & 0\\ \bar{e}_{15} & \bar{e}_{25} & 0\\ 0 & 0 & \bar{e}_{36}\end{bmatrix}_k \begin{Bmatrix}-\dfrac{\partial\Phi}{\partial x}\\ -\dfrac{1}{R}\dfrac{\partial\Phi}{\partial\theta}\\ -\dfrac{\partial\Phi}{\partial z}\end{Bmatrix}_k$$

$$\begin{Bmatrix}D_x\\ D_\theta\\ D_z\end{Bmatrix}_k = \begin{bmatrix}0 & 0 & \bar{e}_{14} & \bar{e}_{15} & 0\\ 0 & 0 & \bar{e}_{24} & \bar{e}_{25} & 0\\ \bar{e}_{31} & \bar{e}_{32} & 0 & 0 & \bar{e}_{36}\end{bmatrix}_k \begin{Bmatrix}\varepsilon_x\\ \varepsilon_y\\ \gamma_{yz}\\ \gamma_{xz}\\ \gamma_{xy}\end{Bmatrix}_k - \begin{bmatrix}\varepsilon_x & \varepsilon_{xy} & 0\\ \varepsilon_{xy} & \varepsilon_y & 0\\ 0 & 0 & \varepsilon_z\end{bmatrix}_k \tag{4a,b}$$

where $\left(\bar{Q}_{ij}\right)^k$ are the transformed stiffness components of the kth layer, $\bar{e}_{ij}^k$ are the transformed piezoelectric moduli, Φ is the applied voltage across the kth layer and ε_x^k, ε_y^k, ε_{xy}^k, ε_z^k are dielectric coefficients of the kth layer.

In-plane stress resultants (N_x, N_θ, $N_{x\theta}$, $N_{\theta x}$), couple resultants (M_x, M_θ, $M_{x\theta}$, $M_{\theta x}$) and transverse shear force resultants (Q_x, Q_θ) can be determined by integration of the relevant stress components over the entire thickness of the panel as below:

$$\begin{Bmatrix}N_x\\ N_{x\theta}\\ Q_x\\ M_x\\ M_{x\theta}\end{Bmatrix} = \int_{-h/2}^{h/2}\begin{Bmatrix}\sigma_x\\ \tau_{x\theta}\\ \tau_{xz}\\ z\,\sigma_x\\ z\,\tau_{x\theta}\end{Bmatrix}\left(1+z\ /\ R\right)dz\,, \qquad \begin{Bmatrix}N_\theta\\ N_{\theta x}\\ Q_\theta\\ M_\theta\\ M_{\theta x}\end{Bmatrix} = \int_{-h/2}^{h/2}\begin{Bmatrix}\sigma_\theta\\ \tau_{\theta x}\\ \tau_{\theta z}\\ z\,\sigma_\theta\\ z\,\tau_{\theta x}\end{Bmatrix}dz \tag{5}$$

It is seen that for a cylindrical panel in general case $N_{x\theta} \neq N_{\theta x}$ and $M_{x\theta} \neq M_{\theta x}$, unless the term z/R is ignored. This is due to the difference in the radii of curvature in two perpendicular directions.

Finally, constitutive equations for general laminated cylindrical panels in terms of displacement and rotation components can be derived as:

$$\begin{Bmatrix}N_x\\ N_{x\theta}\\ Q_x\\ N_\theta\\ N_{\theta x}\\ Q_\theta\\ M_x\\ M_{x\theta}\\ M_\theta\\ M_{\theta x}\end{Bmatrix} = \begin{bmatrix}G_{11} & G_{16} & 0 & A_{12} & A_{16} & 0 & H_{11} & H_{16} & B_{12} & B_{16}\\ G_{61} & G_{66} & 0 & A_{62} & A_{66} & 0 & H_{61} & H_{66} & B_{62} & B_{66}\\ 0 & 0 & K_sG_{55} & 0 & 0 & K_sA_{54} & 0 & 0 & 0 & 0\\ A_{21} & A_{26} & 0 & G'_{22} & G'_{26} & 0 & B_{21} & B_{26} & H'_{22} & H'_{26}\\ A_{61} & A_{66} & 0 & G'_{62} & G'_{66} & 0 & B_{61} & B_{66} & H'_{62} & H'_{66}\\ 0 & 0 & K_sA_{45} & 0 & 0 & K_sG'_{44} & 0 & 0 & 0 & 0\\ H_{11} & H_{16} & 0 & B_{12} & B_{16} & 0 & J_{11} & J_{16} & D_{12} & D_{16}\\ H_{61} & H_{66} & 0 & B_{62} & B_{66} & 0 & J_{61} & J_{66} & D_{62} & D_{66}\\ B_{21} & B_{26} & 0 & H'_{22} & H'_{26} & 0 & D_{21} & D_{26} & J'_{22} & J'_{26}\\ B_{61} & B_{66} & 0 & H'_{62} & H'_{66} & 0 & D_{61} & D_{66} & J'_{62} & J'_{66}\end{bmatrix} \begin{Bmatrix}u_{0,x}\\ v_{0,x}\\ w_{0,x}+\beta_x\\ R^{-1}(v_{0,\theta}+w_0)\\ R^{-1}u_{0,\theta}\\ R^{-1}(w_{0,\theta}-v_0)+\beta_\theta\\ \beta_{x,x}\\ \beta_{\theta,x}\\ R^{-1}\beta_{\theta,\theta}\\ R^{-1}\beta_{x,\theta}\end{Bmatrix} - \begin{Bmatrix}N_x^p\\ N_{x\theta}^p\\ Q_x^p\\ N_\theta^p\\ N_{\theta x}^p\\ Q_\theta^p\\ M_x^p\\ M_{x\theta}^p\\ M_\theta^p\\ M_{\theta x}^p\end{Bmatrix} \tag{6a}$$

$$\begin{Bmatrix} N_x^p \\ N_{x\theta}^p \\ Q_x^p \\ M_x^p \\ M_{x\theta}^p \end{Bmatrix} = \int_{-h/2}^{h/2} \begin{Bmatrix} \bar{e}_{31}.\Phi_z \\ \bar{e}_{36}.\Phi_z \\ \bar{e}_{15}.\Phi_x + \bar{e}_{25}.\Phi_\theta \\ z.\bar{e}_{31}.\Phi_z \\ z.\bar{e}_{36}.\Phi_z \end{Bmatrix} dz + \frac{1}{R}\int_{-h/2}^{h/2} \begin{Bmatrix} z.\bar{e}_{31}.\Phi_z \\ z.\bar{e}_{36}.\Phi_z \\ z.(\bar{e}_{15}.\Phi_x + \bar{e}_{25}.\Phi_\theta) \\ z^2.\bar{e}_{31}.\Phi_z \\ z^2.\bar{e}_{36}.\Phi_z \end{Bmatrix} dz$$

$$\begin{Bmatrix} N_\theta^p \\ N_{\theta x}^p \\ Q_\theta^p \\ M_\theta^p \\ M_{\theta x}^p \end{Bmatrix} = \int_{-h/2}^{h/2} \begin{Bmatrix} \bar{e}_{32}.\Phi_z \\ \bar{e}_{36}.\Phi_z \\ \bar{e}_{14}.\Phi_x + \bar{e}_{24}.\Phi_\theta \\ z.\bar{e}_{32}.\Phi_z \\ z.\bar{e}_{36}.\Phi_z \end{Bmatrix} dz \tag{6b}$$

in which K_s is the shear correction factor and all components of the coefficient matrix can be determined using:

$$(A_{ij}, B_{ij}, D_{ij}, E_{ij}, F_{ij}) = \int_{-h./2}^{h/2} \left(\bar{Q}_{ij}\right)^k (1, z, z^2, z^3, z^4) dz \quad \text{i,j=1,2,4,5,6} \tag{7a}$$

$$\begin{gathered} G_{ij} = A_{ij} + \frac{1}{R}B_{ij}, \quad H_{ij} = B_{ij} + \frac{1}{R}D_{ij}, \quad J_{ij} = D_{ij} + \frac{1}{R}E_{ij}, \\ G'_{ij} = A_{ij} - \frac{1}{R}B_{ij} + \frac{1}{R^2}D_{ij}, \quad H'_{ij} = B_{ij} - \frac{1}{R}D_{ij} + \frac{1}{R^2}E_{ij}, \quad J'_{ij} = D_{ij} - \frac{1}{R}E_{ij} + \frac{1}{R^2}F_{ij}, \end{gathered} \tag{7b}$$

In all presented results 5/6 is considered for the shear correction factor K_s.

The equations of motion can be obtained using the principle of minimum potential energy whereas for the present case yields to[30]:

$$\begin{gathered} \frac{\partial N_x}{\partial x} + \frac{1}{R}\frac{\partial N_{\theta x}}{\partial \theta} = 0, \quad \frac{\partial N_{x\theta}}{\partial x} + \frac{1}{R}\frac{\partial N_\theta}{\partial \theta} + \frac{Q_\theta}{R} = 0 \\ \frac{\partial Q_x}{\partial x} + \frac{1}{R}\frac{\partial Q_\theta}{\partial \theta} - \frac{N_\theta}{R} = -q(x,\theta), \quad \frac{\partial M_x}{\partial x} + \frac{1}{R}\frac{\partial M_{\theta x}}{\partial \theta} - Q_x = 0 \\ \frac{\partial M_{x\theta}}{\partial x} + \frac{1}{R}\frac{\partial M_\theta}{\partial \theta} - Q_\theta = 0 \end{gathered} \tag{8}$$

where $q(x,\theta)$ is the lateral distributed load.

The five equations of motion together with the ten constitutive equations are the complete set of governing equations for static analysis of piezoelectric laminated cylindrical panels. The governing equations consist of a set of partial differential equations in terms of fifteen unknowns, i.e. displacement, rotation and stress resultant components.

Three different types of boundary conditions, i.e. clamped (C), simply supported (S) and free (F) are considered. These boundary conditions in terms of panel parameters are:

-Clamped (C):

$$u_x = u_\theta = w = \beta_x = \beta_\theta = 0 \qquad (at\ x\ \&\ \theta = constant) \tag{9}$$

-Simply supported (S):

$$\begin{gathered} N_{xx} = u_\theta = w = M_{xx} = \beta_\theta = 0 \quad (at\ x = constant) \\ u_x = N_{\theta\theta} = w = \beta_x = M_{\theta\theta} = 0 \quad (at\ \theta = cons\tan t) \end{gathered} \tag{10}$$

-Free (F):

$$\begin{gathered} N_{xx} = N_{x\theta} = Q_x = M_{xx} = M_{x\theta} = 0 \quad (at\ x = constant) \\ N_{\theta x} = N_{\theta\theta} = Q_\theta = M_{\theta x} = M_{\theta\theta} = 0 \quad (at\ \theta = constant) \end{gathered} \tag{11}$$

Once mid-surface displacements and rotations are found from governing equations, one may obtain all strain components through the thickness of the panel using equations (2) and (3). Finally, all stress components within the k^{th} layer of the panel are determined using the stress-strain relations for the same layer and then the stress resultants can be found.

3. Application of the GDQ

The GDQ method is employed to solve the developed differential equations of the laminated piezoelectric cylindrical panels. The essence of the GDQ method is that the partial derivative of a function with respect to a variable is approximated by a weighted sum of function values at all discrete points in that direction. Considering a function *f(x)* with *n* discrete grid points[31], we have

$$\frac{\partial f^m(x)}{\partial x^m}\Big|_{x_i} = \sum_{j=1}^{n} C_{ij}^{(m)} f(x_j) \quad i = 1,2,.....,n \tag{12}$$

where x_j are the discrete points in the variable domain. $f(x_j)$ and $C_{ij}^{(m)}$ are the function values at these points and the related weighting coefficients, respectively. In order to determine the weighting coefficients $C_{ij}^{(m)}$, the Lagrange interpolation basic functions[32, 33] are used as the test functions and explicit formulas for computing the GDQ weighting coefficients are obtained[34],

$$C_{kj}^{(1)} = \frac{P(x_k)}{(x_k - x_j)P(x_j)} \quad k, j = 1,2,...,n \ ; \ k \neq j \tag{13}$$

where,

$$P(x_k) = \prod_{k=1}^{n} (x_k - x_j) \quad k, j = 1,2,...,n \ ; \ k \neq j \tag{14}$$

for first order derivative. For higher order derivatives, one can get iteratively:

$$C_{kj}^{(r)} = r\left[C_{kk}^{(r-1)} C_{kj}^{(1)} - \frac{C_{kj}^{(r-1)}}{(x_k - x_j)} \right] \quad 2 \le r \le n-1 \ ; \ k \neq j \tag{15a}$$

$$C_{kk}^{(r)} = -\sum_{\substack{k=1 \\ k \neq l}}^{n} C_{kl}^{(r)} \quad k = 1,2,...,n, \ 1 \le r \le n-1 \tag{15b}$$

As referred above, the first step to employ the GDQ technique is to discretize the solution domain into $n \times m$ grid points. It means that we assume *n* grid points in the *x* direction and *m* grid points in the θ direction. Although the simplest procedure for discretization of the domain is to select equally spaced points, it is shown[34] that one of the best options for obtaining grid points is zeros of the well-known Chebyshev polynomials:

$$\begin{aligned} x_i &= \frac{a}{2}\left[1 - \cos\left(\frac{i-1}{n_x - 1}\pi\right)\right], \quad i = 1,2,...,n \\ \theta_i &= \frac{\alpha}{2}\left[1 - \cos\left(\frac{i-1}{n_\theta - 1}\pi\right)\right], \quad i = 1,2,...,m \end{aligned} \tag{16}$$

where *a* and α are geometric parameters of the panel shown in Figure 1. The next step is to discretize the governing equations based on the definition given in equation (12). Thus, the discretized form of the governing equations at a sample grid point (*i,j*) can be written as:

$$\begin{aligned} &N_{xx}(x_i,\theta_j) - G_{11}(x_i)\sum_{k=1}^{n} C_{ik} u_0(x_k,\theta_j) - G_{16}(x_i)\sum_{k=1}^{n} C_{ik} v_0(x_k,\theta_j) \\ &-\frac{A_{12}}{R}\left(w_0(x_i,\theta_j) + \sum_{l=1}^{m} \overline{C}_{jl} v_0(x_i,\theta_l) \right) - \frac{A_{16}}{R}\sum_{l=1}^{m} \overline{C}_{jl} u_0(x_i,\theta_l) - H_{11}(x_i)\sum_{k=1}^{n} C_{ik}\beta_x(x_k,\theta_j) \\ &-H_{16}(x_i)\sum_{k=1}^{n} C_{ik}\beta_\theta(x_k,\theta_j) - \frac{B_{12}}{R}\sum_{l=1}^{m} \overline{C}_{jl}\beta_\theta(x_i,\theta_l) - \frac{B_{16}}{R}\sum_{l=1}^{m} \overline{C}_{jl}\beta_x(x_i,\theta_l) = N_{xx}^P \\ &N_{x\theta}(x_i,\theta_j) - G_{61}(x_i)\sum_{k=1}^{n} C_{ik} u_0(x_k,\theta_j) - G_{66}(x_i)\sum_{k=1}^{n} C_{ik} v_0(x_k,\theta_j) \\ &-\frac{A_{62}}{R}\left(w_0(x_i,\theta_j) + \sum_{l=1}^{m} \overline{C}_{jl} v_0(x_i,\theta_l) \right) - \frac{A_{66}}{R}\sum_{l=1}^{m} \overline{C}_{jl} u_0(x_i,\theta_l) - H_{61}(x_i)\sum_{k=1}^{n} C_{ik}\beta_x(x_k,\theta_j) \\ &-H_{66}(x_i)\sum_{k=1}^{n} C_{ik}\beta_\theta(x_k,\theta_j) - \frac{B_{62}}{R}\sum_{l=1}^{m} \overline{C}_{jl}\beta_\theta(x_i,\theta_l) - \frac{B_{66}}{R}\sum_{l=1}^{m} \overline{C}_{jl}\beta_x(x_i,\theta_l) = N_{x\theta}^P \end{aligned}$$

$$Q_x\left(x_i,\theta_j\right)-K_sA_{54}\left(R^{-1}\left[\sum_{l=1}^{m}\overline{C}_{jl}w_0\left(x_i,\theta_l\right)-v_0\left(x_i,\theta_j\right)\right]+\beta_\theta\left(x_i,\theta_j\right)\right)$$

$$-K_sG_{55}\left(x_i\right)\left(\sum_{k=1}^{n}C_{ik}w_0\left(x_k,\theta_j\right)+\beta_x\left(x_i,\theta_j\right)\right)=Q_x^P$$

$$N_{\theta\theta}\left(x_i,\theta_j\right)-A_{21}\left(x_i\right)\sum_{k=1}^{n}C_{ik}u_0\left(x_k,\theta_j\right)-A_{26}\left(x_i\right)\sum_{k=1}^{n}C_{ik}v_0\left(x_k,\theta_j\right)$$

$$-\frac{G'_{22}}{R}\left(w_0\left(x_i,\theta_j\right)+\sum_{l=1}^{m}\overline{C}_{jl}v_0\left(x_i,\theta_l\right)\right)-\frac{G'_{26}}{R}\sum_{l=1}^{m}\overline{C}_{jl}u_0\left(x_i,\theta_l\right)-B_{21}\left(x_i\right)\sum_{k=1}^{n}C_{ik}\beta_x\left(x_k,\theta_j\right)$$

$$-B_{26}\left(x_i\right)\sum_{k=1}^{n}C_{ik}\beta_\theta\left(x_k,\theta_j\right)-\frac{H'_{22}}{R}\sum_{l=1}^{m}\overline{C}_{jl}\beta_\theta\left(x_i,\theta_l\right)-\frac{H'_{26}}{R}\sum_{l=1}^{m}\overline{C}_{jl}\beta_x\left(x_i,\theta_l\right)=N_{\theta\theta}^P$$

$$N_{\theta x}\left(x_i,\theta_j\right)-A_{61}\left(x_i\right)\sum_{k=1}^{n}C_{ik}u_0\left(x_k,\theta_j\right)-A_{66}\left(x_i\right)\sum_{k=1}^{n}C_{ik}v_0\left(x_k,\theta_j\right)$$

$$-\frac{G'_{62}}{R}\left(w_0\left(x_i,\theta_j\right)+\sum_{l=1}^{m}\overline{C}_{jl}v_0\left(x_i,\theta_l\right)\right)-\frac{G'_{66}}{R}\sum_{l=1}^{m}\overline{C}_{jl}u_0\left(x_i,\theta_l\right)-B_{61}\left(x_i\right)\sum_{k=1}^{n}C_{ik}\beta_x\left(x_k,\theta_j\right)$$

$$-B_{66}\left(x_i\right)\sum_{k=1}^{n}C_{ik}\beta_\theta\left(x_k,\theta_j\right)-\frac{H'_{62}}{R}\sum_{l=1}^{m}\overline{C}_{jl}\beta_\theta\left(x_i,\theta_l\right)-\frac{H'_{66}}{R}\sum_{l=1}^{m}\overline{C}_{jl}\beta_x\left(x_i,\theta_l\right)=N_{\theta x}^P$$

$$Q_\theta\left(x_i,\theta_j\right)-K_sG'_{44}\left(R^{-1}\left[\sum_{l=1}^{m}\overline{C}_{jl}w_0\left(x_i,\theta_l\right)-v_0\left(x_i,\theta_j\right)\right]+\beta_\theta\left(x_i,\theta_j\right)\right)$$

$$-K_sA_{45}\left(x_i\right)\left(\sum_{k=1}^{n}C_{ik}w_0\left(x_k,\theta_j\right)+\beta_x\left(x_i,\theta_j\right)\right)=Q_\theta^P$$

$$M_{xx}\left(x_i,\theta_j\right)-H_{11}\left(x_i\right)\sum_{k=1}^{n}C_{ik}u_0\left(x_k,\theta_j\right)-H_{16}\left(x_i\right)\sum_{k=1}^{n}C_{ik}v_0\left(x_k,\theta_j\right)$$

$$-\frac{B_{12}}{R}\left(w_0\left(x_i,\theta_j\right)+\sum_{l=1}^{m}\overline{C}_{jl}v_0\left(x_i,\theta_l\right)\right)-\frac{B_{16}}{R}\sum_{l=1}^{m}\overline{C}_{jl}u_0\left(x_i,\theta_l\right)-J_{11}\left(x_i\right)\sum_{k=1}^{n}C_{ik}\beta_x\left(x_k,\theta_j\right)$$

$$-J_{16}\left(x_i\right)\sum_{k=1}^{n}C_{ik}\beta_\theta\left(x_k,\theta_j\right)-\frac{D_{12}}{R}\sum_{l=1}^{m}\overline{C}_{jl}\beta_\theta\left(x_i,\theta_l\right)-\frac{D_{16}}{R}\sum_{l=1}^{m}\overline{C}_{jl}\beta_x\left(x_i,\theta_l\right)=M_{xx}^P$$

$$M_{x\theta}\left(x_i,\theta_j\right)-H_{61}\left(x_i\right)\sum_{k=1}^{n}C_{ik}u_0\left(x_k,\theta_j\right)-H_{66}\left(x_i\right)\sum_{k=1}^{n}C_{ik}v_0\left(x_k,\theta_j\right)$$

$$-\frac{B_{62}}{R}\left(w_0\left(x_i,\theta_j\right)+\sum_{l=1}^{m}\overline{C}_{jl}v_0\left(x_i,\theta_l\right)\right)-\frac{B_{66}}{R}\sum_{l=1}^{m}\overline{C}_{jl}u_0\left(x_i,\theta_l\right)-J_{61}\left(x_i\right)\sum_{k=1}^{n}C_{ik}\beta_x\left(x_k,\theta_j\right)$$

$$-J_{66}\left(x_i\right)\sum_{k=1}^{n}C_{ik}\beta_\theta\left(x_k,\theta_j\right)-\frac{D_{62}}{R}\sum_{l=1}^{m}\overline{C}_{jl}\beta_\theta\left(x_i,\theta_l\right)-\frac{D_{66}}{R}\sum_{l=1}^{m}\overline{C}_{jl}\beta_x\left(x_i,\theta_l\right)=N_{x\theta}^P$$

$$M_{\theta\theta}\left(x_i,\theta_j\right)-B_{21}\left(x_i\right)\sum_{k=1}^{n}C_{ik}u_0\left(x_k,\theta_j\right)-B_{26}\left(x_i\right)\sum_{k=1}^{n}C_{ik}v_0\left(x_k,\theta_j\right)$$

$$-\frac{H'_{22}}{R}\left(w_0\left(x_i,\theta_j\right)+\sum_{l=1}^{m}\overline{C}_{jl}v_0\left(x_i,\theta_l\right)\right)-\frac{H'_{26}}{R}\sum_{l=1}^{m}\overline{C}_{jl}u_0\left(x_i,\theta_l\right)-D_{21}\left(x_i\right)\sum_{k=1}^{n}C_{ik}\beta_x\left(x_k,\theta_j\right)$$

$$-D_{26}\left(x_i\right)\sum_{k=1}^{n}C_{ik}\beta_\theta\left(x_k,\theta_j\right)-\frac{J'_{22}}{R}\sum_{l=1}^{m}\overline{C}_{jl}\beta_\theta\left(x_i,\theta_l\right)-\frac{J'_{26}}{R}\sum_{l=1}^{m}\overline{C}_{jl}\beta_x\left(x_i,\theta_l\right)=M_{\theta\theta}^P$$

$$
\begin{aligned}
&M_{\theta x}\left(x_i,\theta_j\right)-B_{61}\left(x_i\right)\sum_{k=1}^{n}C_{ik}u_0\left(x_k,\theta_j\right)-B_{66}\left(x_i\right)\sum_{k=1}^{n}C_{ik}v_0\left(x_k,\theta_j\right)\\
&-\frac{H'_{62}}{R}\left(w_0\left(x_i,\theta_j\right)+\sum_{l=1}^{m}\overline{C}_{jl}v_0\left(x_i,\theta_l\right)\right)-\frac{H'_{66}}{R}\sum_{l=1}^{m}\overline{C}_{jl}u_0\left(x_i,\theta_l\right)-D_{61}\left(x_i\right)\sum_{k=1}^{n}C_{ik}\beta_x\left(x_k,\theta_j\right)\\
&-D_{66}\left(x_i\right)\sum_{k=1}^{n}C_{ik}\beta_\theta\left(x_k,\theta_j\right)-\frac{J'_{62}}{R}\sum_{l=1}^{m}\overline{C}_{jl}\beta_\theta\left(x_i,\theta_l\right)-\frac{J'_{66}}{R}\sum_{l=1}^{m}\overline{C}_{jl}\beta_x\left(x_i,\theta_l\right)=M^{P}_{\theta x}\\
&\sum_{k=1}^{n}C_{ik}N_{xx}\left(x_k,\theta_j\right)+\frac{1}{R}\sum_{l=1}^{m}\overline{C}_{jl}N_{\theta x}\left(x_i,\theta_l\right)=0\\
&\sum_{k=1}^{n}C_{ik}N_{x\theta}\left(x_k,\theta_j\right)+\frac{1}{R}\left(\sum_{l=1}^{m}\overline{C}_{jl}N_{\theta}\left(x_i,\theta_l\right)+Q_{\theta}\left(x_i,\theta_j\right)\right)=0\\
&\sum_{k=1}^{n}C_{ik}Q_x\left(x_k,\theta_j\right)+\frac{1}{R}\left(\sum_{l=1}^{m}\overline{C}_{jl}Q_{\theta}\left(x_i,\theta_l\right)-N_{\theta}\left(x_i,\theta_j\right)\right)=-q(x,\theta)\\
&\sum_{k=1}^{n}C_{ik}M_x\left(x_k,\theta_j\right)+\frac{1}{R}\sum_{l=1}^{m}\overline{C}_{jl}M_{\theta x}\left(x_i,\theta_l\right)-Q_x\left(x_i,\theta_j\right)=0\\
&\sum_{k=1}^{n}C_{ik}M_{x\theta}\left(x_k,\theta_j\right)+\frac{1}{R}\sum_{l=1}^{m}\overline{C}_{jl}M_{\theta}\left(x_i,\theta_l\right)-Q_{\theta}\left(x_i,\theta_j\right)=0
\end{aligned}
\tag{17}
$$

Following the procedure leads to a system of 15($n\times m$) algebraic equations with the same number of unknowns.

The last step is to apply boundary conditions (10-12) to the obtained algebraic equations. Considering the fact that five of the fifteen unknown parameters vanish at each boundary node for any type of boundary conditions, the relevant unknowns should be removed from the equations.

4. Results and Discussion

The presented algorithm is employed to solve the governing equations of static analysis for laminated orthotropic cylindrical panels integrated with piezoelectric layers. In this study the effects of different types of boundary conditions are investigated. Three general types of loadings are considered: electrical, mechanical and electromechanical. A plate with SCFS boundary conditions means that sides 1, 2, 3, 4 (see Figure 1) are simply supported, clamped, free and simply supported, respectively.

Table 1. Normalized induced transverse displacement ($\overline{w}=\frac{10wE_2}{S^4q_0h_c}$, q_0=1) of infinitely long cylindrical panel with one composite layer

$S=R/h_c$	$\Phi_0=0$		$\Phi_0=100$	
	Chen *et al.*[16]	Present work	Chen *et al.*[16]	Present work
10	0.1120	0.1160	-0.0340	-0.0345
50	0.0754	0.0764	0.0481	0.0487
100	0.0740	0.0754	0.0604	0.0613

At first, the efficiency and the accuracy of the present method are demonstrated. The normalized transverse central deflections for a simply supported infinitely long cylindrical panel subjected to sinusoidal distributed mechanical and electrical loading are compared with those of exact elasticity solution for a shell strip having piezoelectric layers in Table 1. The variations of deflection with three values of ($S=R/h_c$) are studied where h_c is the composite layer thickness. To model a long simply supported panel, the length of the panel is considered to be extremely large and the boundary conditions are considered to be SFSF.

The piezoelectric layers are assumed to be embedded on the top and the bottom surfaces of the panel. The top and the bottom layers are taken as the actuator and the sensor, respectively. The middle layer is an orthotropic material with the fiber orientation angle of 90°. It should be noted that the fiber angles of laminates are measured relative to the panel axis. The thickness ratio of the piezoelectric layer to the composite layer is $h_p/h_c=0.01$, the panel radius is R=1 and the panel total angle is equal to $\alpha=\pi/3$. The Piezoelectric layers are assumed to be elastically isotropic and uniaxially polarized with the material properties of:

$$
\begin{aligned}
&E=2GPa \quad \upsilon=0.29 \quad e_{31}=0.046(C/m^2)\\
&\varepsilon_{11}=\varepsilon_{22}=\varepsilon_{rr}=\varepsilon_{\theta\theta}=0.106E-9(F/m)
\end{aligned}
\tag{18}
$$

The material properties of the graphite/epoxy composite layers are:

$$E_1 = 172GPa \quad E_2 = 6.9GPa \quad \upsilon_{12} = \upsilon_{13} = 0.25$$
$$G_{12} = 3.4GPa \quad G_{23} = 1.4GPa \tag{19}$$

The electromechanical loading functions are expressed as: $q = q_0 \sin(\frac{\pi\theta}{\alpha})$, $\Phi = \Phi_0 \sin(\frac{\pi\theta}{\alpha})$ where q_0 and Φ_0 are the peak value. The voltage is applied to the upper surface of the actuator, while the voltage of the actuator interface and the sensor surfaces are assumed to be zero. It is seen that the predicted normalized transverse displacements are in good agreement with those reported by Ref.[16].

Table 2. Normalized induced transverse displacement ($\overline{w} = \frac{10wE_2}{S^4 q_0 h_c}$, q_0=1) of infinitely long cylindrical panel with three composite layers

$S=R/h_c$	Φ_0 =0		Φ_0 =100	
	Chen *et al.*[16]	Present work	Chen *et al.*[16]	Present work
10	0.1440	0.1511	-0.0227	-0.0230
50	0.0808	0.0819	0.0518	0.0522
100	0.0785	0.0797	0.0641	0.0650

Similar results are tabulated in Table 2 for a different layup of the middle composite layers. The middle layers are made of equal thickness plies with the stacking sequence of[90/0/90]. Again good agreements are achieved.

To show the capability of the GDQ method in accurately predicting stresses, a fully simply supported cylindrical panel subjected to doubly sinusoidal loading on the upper surface

($q_{(x,\theta)} = q_0 \times \sin(\pi x'/a)\sin(\pi\theta/\alpha),\ x' = x + a/2$)

is considered. Material properties of the panel are: $E_1/E_2 = 25, G_{12}/E_2 = G_{13}/E_2 = 0.5$, $G_{23}/E_2 = 0.2$, $\upsilon_{12} = 0.25$ and the geometry parameters are set to be: (a=4, R=1, $\alpha=\pi/4$, $S=R/h=50$). The normalized central deflection and stresses for both symmetric (90/0/90) and asymmetric cross ply (0/90) layups are presented in Table 3. In both cases the layers are of equal thickness. The normalized transverse deflection and stresses are defined as follows:

$$\begin{aligned} &w^*(0,\alpha/2),\ \sigma_{xx}^1{}^* = \sigma_{xx}{}^*(0,\alpha/2,h/2) \\ &\sigma_{xx}^2{}^* = \sigma_{xx}{}^*(0,\alpha/2,-h/2) \\ &\sigma_{yy}^1{}^* = \sigma_{yy}{}^*(0,\alpha/2,h/2) \\ &\sigma_{yy}^2{}^* = \sigma_{yy}{}^*(0,\alpha/2,-h/2) \\ &\sigma_{xy}^1{}^* = \sigma_{xy}{}^*(a/2,0,h/2) \\ &\sigma_{xy}^2{}^* = \sigma_{xy}{}^*(a/2,0,-h/2) \end{aligned} \tag{20}$$

where:

$$w^* = \frac{10wE_1}{q_0 h S^3}, \quad \sigma_{ij}^* = \frac{10\sigma_{ij}}{q_0 S^2} \tag{21}$$

Included in the table are also benchmarks results of three-dimensional elasticity analysis[35], closed form solution of higher order zigzag theory[36] and finite element analysis[30]. It is demonstrated that the obtained GDQ results are in good agreement with the other solutions.

Table 3. Normalized deflection and stress of simply supported cylindrical panel under sinusoidal distributed mechanical loading

Model	w^*	σ^{1*}_{xx}	σ^{2*}_{xx}	σ^{1*}_{yy}	σ^{2*}_{yy}	σ^{1*}_{xy}	σ^{2*}_{xy}
				[90/0/90]			
3D Elasticity[35]	0.5495	0.0712	-0.0225	3.930	-3.987	0.0118	0.0760
FEM[30]	0.5458	0.0711	-0.0214	3.9489	-3.9555	0.0114	0.0765
Closed Form[36]	0.5486	0.0710	-0.0217	3.9265	-3.9870	0.0123	0.0764
GDQ	0.5459	0.0712	-0.0213	3.9434	-3.9625	0.0114	0.0765
				[0°/90°]			
3D Elasticity[35]	2.242	0.2189	1.61	8.937	-0.9670	0.0784	0.3449
FEM[30]	2.2586	0.2211	1.6169	9.0939	-0.9601	0.0767	0.3501
Closed Form[36]	2.2372	0.2187	1.6051	8.9543	-0.9615	0.0784	0.3444
GDQ	2.2644	0.2211	1.6253	9.1102	-0.9647	0.0769	0.3502

To demonstrate the capability of the developed algorithm to deal with arbitrary boundary conditions and either electrical or mechanical loadings, an illustrative example is taken up. A piezoelectric cylindrical panel with a length and radius of a=R=1m, a total angle of $\alpha = 1Rad$ and thickness of h=0.1m is considered. The complete set of results can be used as benchmarks in future studies.

In the following results, the panels are considered to be composed of PZT-4 and polyvinyledene fluoride (PVDF) polarized along the radial direction. The laminates layup and the direction of polarization of the piezoelectric laminates are shown schematically in Figure 2. The individual layers are taken to be of equal thickness. The elastic and piezoelectric properties of piezoelectric material are also given in Table 4[37]. Three types of uniform loading are considered for panels as: electrical, mechanical and electromechanical by setting q=q_0 and/or Φ=Φ_0 which are applied to the upper surface.

Table 4. Material properties of piezoelectric layers

Property	Heyliger, Saravanos[37]	
	PZT-4	PVDF
$E_1(GPa)$	81.3	237.0
$E_2(GPa)$	81.3	23.2
$E_3(GPa)$	64.5	10.5
ν_{12}	0.329	0.154
ν_{13}	0.432	0.178
ν_{23}	0.432	0.177
$G_{23}(GPa)$	25.6	2.15
$G_{13}(GPa)$	25.6	4.4
$G_{12}(GPa)$	30.6	6.43
$e_{31}\ (C/m^2)$	-5.2	-0.13
$e_{32}\ (C/m^2)$	-5.2	-0.14
$e_{33}\ (C/m^2)$	15.08	-0.28
$e_{24}\ (C/m^2)$	12.72	-0.01
$e_{15}\ (C/m^2)$	12.72	-0.01

4.1. Electrical Loading

In order to show the convergence of the present work, the non-dimensional deflection of the piezoelectric panel is presented for different types of boundary conditions in Figs. 3 through 5. The polarization of PVDF layers (see Figure 2) are reversed and the electrical/mechanical parameters of the loading are considered to be $(\Phi_0 = 100, q_0 = 0)$. The deflections are reported on the central circumferential line of the panel ($\theta/\alpha = 0.5$) and are calculated from expression $w^* = w\left(\frac{E_2 e_{31}}{10\Phi_0}\right)$ in terms of PZT-4 properties. The boundary conditions of the panels are *FCFF, FCCF* and *CCFC* in Figs. 3-5, respectively. It is obvious that the free type boundary conditions exhibit the worst convergence characteristic than the others. It is found that the use of seventeen grid points in the x and θ directions respectively can provide accurate numerical results. This guarantees faster rate of convergence of the method for other types of boundary conditions.

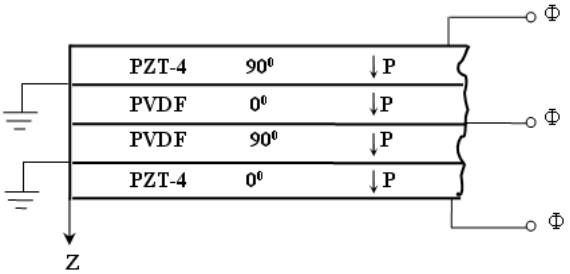

Figure 2. Laminates layup and electrical loading of piezoelectric layers

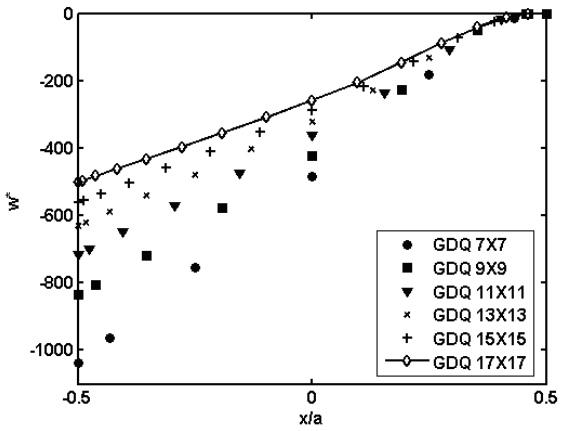

Figure 3. Normalized deflection w^* of cantilever piezoelectric laminated cylindrical panels under electric loading $(\Phi_0 = 100, q_0 = 0)$ at $\theta/\alpha = 0.5$

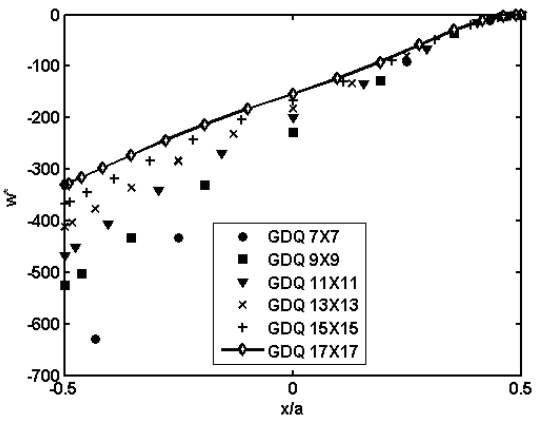

Figure 4. Normalized deflection w^* of *FCCF* piezoelectric laminated cylindrical panels under electric loading $(\Phi_0 = 100, q_0 = 0)$ at $\theta/\alpha = 0.5$

After performing the convergence studies, new results for panels with different set of boundary conditions are developed. Figs. 6 and 7 show the dimensionless central deflection w^* of the piezoelectric laminated cylindrical panel with various boundary conditions along x axis at $\theta/\alpha = 0.5$. It is realized that the solution characteristics of the method is dependent on the boundary conditions. It is also seen that the locations of the maximum deflections are dependent on the type of boundary conditions. Although, the maximum deflection naturally occurs at the center of the fully simply supported panel, its location is not evident for other boundary conditions.

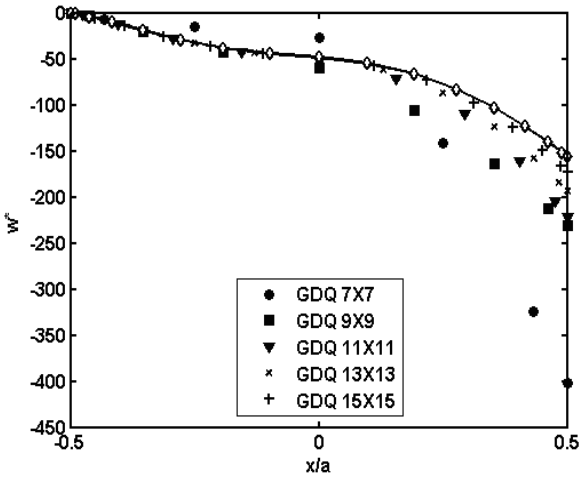

Figure 5. Normalized deflection w^* of CCFC piezoelectric laminated cylindrical panels under electric loading $(\Phi_0 = 100, q_0 = 0)$ at $\theta/\alpha = 0.5$

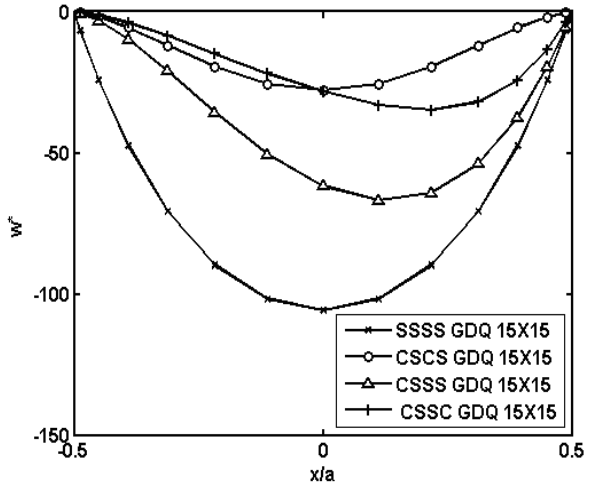

Figure 6. Normalized deflection w^* of piezoelectric laminated cylindrical panels with various boundary conditions under electrical loading $(\Phi_0 = 100, q_0 = 0)$ at $\theta/\alpha = 0.5$

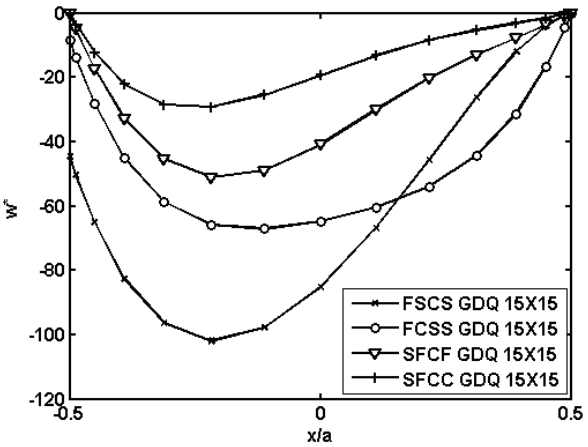

Figure 7. Non-dimensional deflection w^* of piezoelectric laminated cylindrical panels with free edges under electrical loading $(\Phi_0 = 100, q_0 = 0)$ at $\theta/\alpha = 0.5$

4.2. Mechanical Loading

The normalized transverse deflection $\left(w^{**}\right)$ of the piezoelectric laminated cylindrical panel under uniform lateral mechanical loading $(\Phi_0 = 0, q_0 = 100)$ is illustrated in Figs. 8 and 9. The normalized deflection is defined as $w^{**} = 1000w\left(\frac{E_2 h^3}{a^4 q_0}\right)$ in terms of PZT-4 properties. Again various boundary conditions are considered and the deflection of panel is reported on the central circumferential line. The results show that clamped edges effectively reduce the deflection especially while they are adjacent to free edges in comparison to opposite free and clamped sides.

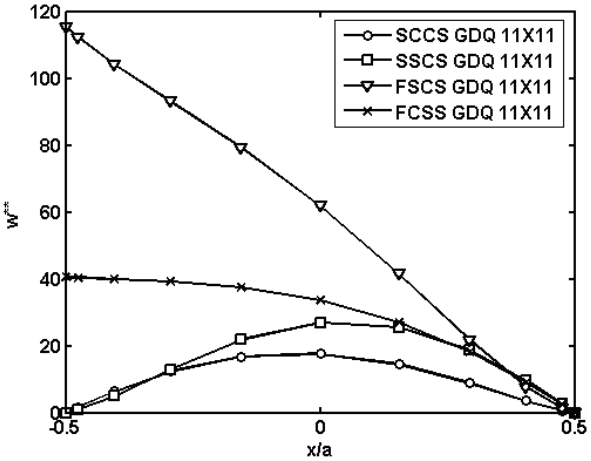

Figure 8. Non-dimensional deflection w^{**} of piezoelectric laminated cylindrical panels with free edges under mechanical loading $(\Phi_0 = 0, q_0 = 100)$ at $\theta/\alpha = 0.5$

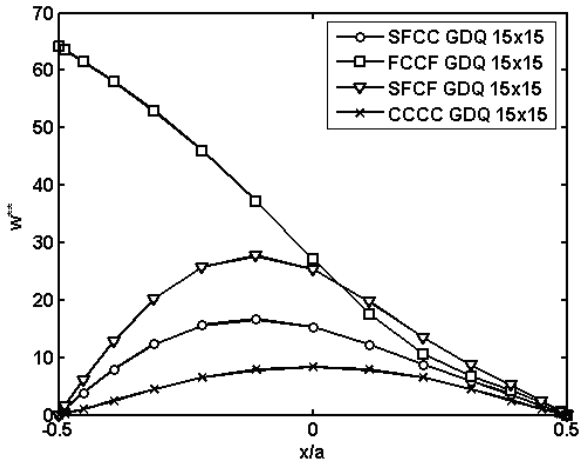

Figure 9. Normalized deflection w^{**} of piezoelectric laminated cylindrical panels with various boundary conditions under mechanical loading $(\Phi_0 = 0, q_0 = 100)$ at $\theta/\alpha = 0.5$

4.3. Electromechanical Loading

The last part of the results is dealt with the general type of electromechanical loading $(\Phi_0 = 100, q_0 = 100)$. Figure 10 depicts effects of the aforementioned boundary conditions on the non-dimensional deflection $\left(w^*\right)$ of the piezoelectric laminated cylindrical panel under this type of loading. The normalized transverse deflection is also expressed in terms of the piezoelectric material properties as $w^* = w\left(\frac{E_2 e_{31}}{10\Phi_0}\right)$.

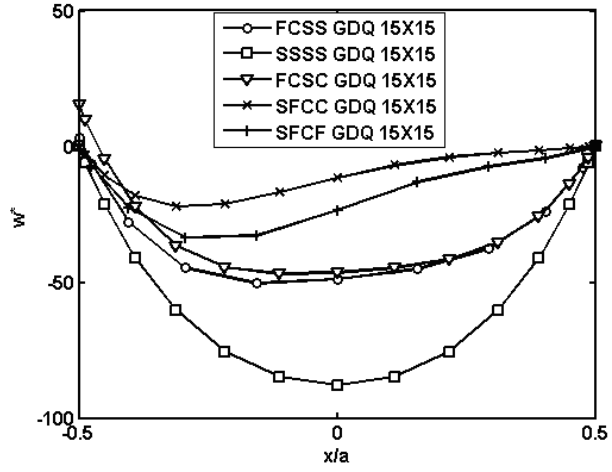

Figure 10. Normalized deflection w^* of piezoelectric laminated cylindrical panels with various boundary conditions under electromechanical loading $(\Phi_0 = 100, q_0 = 100)$ at $\theta/\alpha = 0.5$

The present method is capable of predicting all variables including displacements, rotations and stress resultants with the same order of accuracy. To clarify it, the stress and moment resultants of the piezoelectric laminated cylindrical panel under electromechanical loading are determined. Figs. 11 and 12 illustrate the non-dimensional stress (N_x^*, N_θ^*) and moment resultants (M_x^*, M_θ^*), respectively. The resultants are nondimensionalized according to the equations $N^* = \frac{N}{e_{31}\Phi_0}, M^* = \frac{M}{e_{31}\Phi_0 a}$, where e_{31} is the PZT-4 property. It can be seen that the largest stress resultants occur in the panels having SSSS boundary condition. On the other hand, the stress resultants are at their lowest value for the CCCC case.

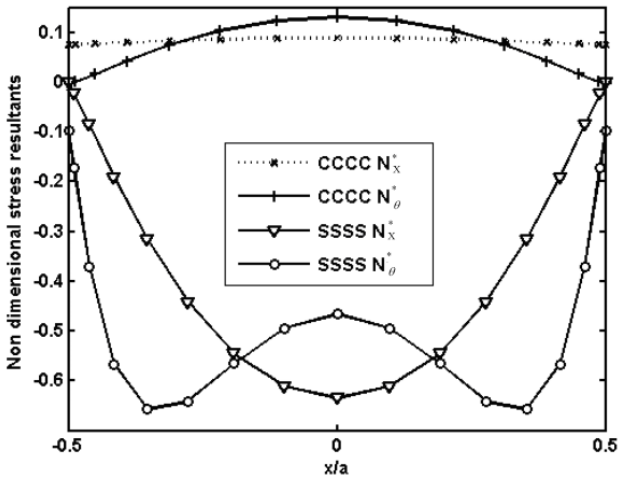

Figure 11. Non-dimensional stress resultants N_x^*, N_θ^* of piezoelectric laminated cylindrical panels under electromechanical loading $(\Phi_0 = 100, q_0 = 100)$ at $\theta/\alpha = 0.5$

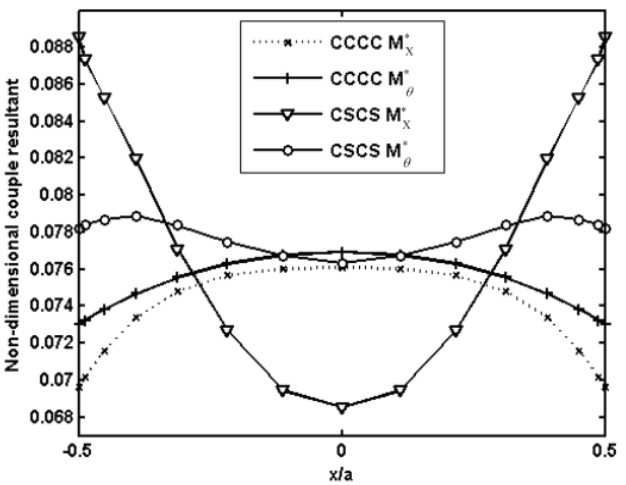

Figure 12. Normalized moment resultants M_x^*, M_θ^* of piezoelectric laminated cylindrical panels under electromechanical loading $(\Phi_0 = 100, q_0 = 100)$ at $\theta/\alpha = 0.5$

5. Conclusions

The applicability and efficiency of the GDQ method are investigated for static analysis of piezoelectric laminated cylindrical panels. The procedure permits a systematic and a straightforward modeling of mixed boundary conditions. Numerical predictions are presented for deflection, stresses and resultant forces with different types of boundary and

various numbers of grid points. Of particular interests in this study are panels with free edges and general electromechanical loading which similar results are not found in the open literature. Presence of all parameters including displacements, rotations and stress resultants in the governing equations provides a simple procedure to handle any boundary conditions without any difficulty. Furthermore, it results in the same order of accuracy for all parameters including stress components.

REFERENCES

[1] Tzou HS, Zhong JP.: Linear theory of piezoelectric shell vibrations. J. Sound Vib. 175(1), 77–88 (1994).

[2] Benjeddou A.: Advances in piezoelectric finite element modelling of adaptive structural elements: a survey. Comput. Struct. 76(1), 347–63 (2000).

[3] Kapuria S, Sengupta S, Dumir PC.: Three-dimensional solution for simply-supported piezoelectric cylindrical shell for axisymmetric load. Comput. Meth. Appl. Mech. Eng. 140(1-2), 139–55 (1997).

[4] Robbins DH, Reddy JN.: Analysis of piezoelectrically actuated beams using a layer-wise displacement theory. Comput. Struct. 41, 265–79 (1991).

[5] Ossadzow-David C, Touratier M.: A mixed model for adaptive composite plates with piezoelectric for anisotropic actuation. Compos. Sci. Technol. 64, 2121–2137 (2004).

[6] Hussein MM and Heyliger P.: Three-dimensional vibrations of layered piezoelectric cylinders. J. Eng. Mech. 124, 1294–8 (1998).

[7] Chen CQ, Shen YP.: Piezothermoelasticity analysis for a cylindrical shell under the state of axisymmetric deformation. Int. J. Eng. Sci. 34(14), 1585–600 (1996).

[8] Bernadou M, Haenel C.: Modelization and numerical approximation of piezoelectric thin shells Part 1: The continuous problems. Comput. Meth. Appl. Mech. Eng. 192, 4003–43 (2003).

[9] Tzou HS, Zhong JP.: Electromechanics and vibrations of piezoelectric shell distributed systems. J. Dyn. Syst. Meas. Contr. 115(3), 506–517 (1993).

[10] Pinto Carreia IF, Mota Soares CM, Mota Soares CA.: Analysis of piezolaminated axisymmetric shell: a semi analytical higher order model. In: Computational Methods for Shell and Spatial Structures, Proc. IASS-IACM, Athens, p. 1–19 (2000).

[11] Heyliger P, Pei KC, Saravanos D.: Layerwise mechanics and finite element model for laminated piezoelectric shell, Journal of AIAA, 34, 2353–60 (1996).

[12] Dumir PC, Dube GP, Kapuria S.: Exact Piezoelectric solution of simply-supported orthotropic circular cylindrical panel in cylindrical bending. Int. J. Solids Struct. 6, 685-702 (1997).

[13] Saviz MR, Shakeri M, Yas MH.: Electroelastic fields in a layered piezoelectric cylindrical shell under dynamic load. Smart Mater. Struct. 16, 1683–1695 (2007).

[14] Kogl M, Gaul L.: A boundary element method for transient piezoelectric analysis. Engineering 1. Eng. Anal. Boundary Elem. 24, 591–598 (2000).

[15] Ray MC, Reddy JN.: Active control of laminated cylindrical shells using piezoelectric fiber reinforced composites. Compos. Sci. Technol. 65, 1226–1236 (2005).

[16] Chen CQ, Shen YP, Wang XM.: Exact Solution of orthotropic cylindrical shell with piezoelectric layers under cylindrical bending. Int. J. Solids Struct. 33(30), 4481-4494 (1996).

[17] Kapuria S, Kumari P, Nath JK. Analytical piezoelasticity solution for vibration of piezoelectric laminated angle-ply circular cylindrical panels. J. Sound Vib. 324, 832–849 (2009).

[18] Daneshmehr AR, Shakeri M.: Three-Dimensional Elasticity Solution of Cross-Ply Shallow and Non-Shallow Panels with Piezoelectric Sensors under Dynamic Load. Compos. Struct. 80, 429–439 (2007).

[19] Sedighi MR, Shakeri M.: A three-dimensional elasticity solution of functionally graded piezoelectric cylindrical panels. Int. J. Solids Struct. 18, 1-12 (2009).

[20] Jianqiao Y.: New approach for the bending problem of shallow shell by the boundary element Method. Appl. Math. Modell. 12(5), 467-470 (1988).

[21] Ramesh G, Krishnamoorthy CS.: Geometrically non-linear analysis of plates and shallow shells by dynamic relaxation. Comput. Meth. Appl. Mech. Eng. 123, 15-32 (1995).

[22] Abouhamza M, Aghdam MM., Alijani F.: Bending analysis of symmetrically laminated cylindrical panels using the extended Kantorovich Method. Mech. Adv. Mater. Struct. 14(7), 523-530 (2007).

[23] Alavi SM, Aghdam MM, Eftekhari SA.: Three-dimensional elasticity analysis of thick rectangular laminated composite plates using Meshless Local Petrov-Galerkin (MLPG) method. AMM. 5, 331-338 (2006).

[24] Malekzadeh P, Farid M, Zahedinejad P, Karami G.: Three-dimensional free vibration analysis of thick cylindrical shells resting on two-parameter elastic supports. J. Sound Vib. 313(3), 655-675 (2008).

[25] Malekzadeh P, Farid M, Zahedinejad P.: A three-dimensional layerwise-differential quadrature free vibration analysis of laminated cylindrical shells. Int. J. Press. Vessels Pip. 85(7), 450-458 (2008).

[26] Liu FL, Liew KM.: Differential cubature method for static solutions of arbitrarily shaped thick plates. Int. J. Solids Struct. 35(28-29), 3655–3674 (1998).

[27] Shu C, Du H.: Implementation of clamped and simply supported boundary conditions in the GDQ free vibration analysis of beams and plates. Int. J. Solids Struct. 34(7), 819-35 (1997).

[28] Reddy JN.: On laminated composite plates with integrated sensors and actuators. Eng. Struct. 21, 568–593 (1999).

[29] Toorani MH, Lakis AA. General equations of anisotropic plates and shells including transverse shear deformations,

Rotary inertia and initial curvature effects. J. Sound Vib. 237(4), 561-615 (2000).

[30] Reddy JN.: Mechanics of laminated composite plates and shells: theory and analysis. 2nd ed. Boca Raton: CRC Press, (2004).

[31] Civan F, Sliepcevich CM.: Differential quadrature for multidimensional problems. J. Math. Anal. Appl. 101, 423-443 (1984).

[32] Shu C, Richards BE.: Parallel simulation of incompressible viscous flows by generalized differential quadrature. Comput. Syst. Eng. 3, 271-281 (1992).

[33] Bert CW, Wang X, Striz AG.: Differential quadrature for static and free vibrational analysis of anisotropic plates. Int. J. Solids Struct. 30, 1737-1744 (1993).

[34] Shu C, Richards BE.: Application of generalized differential quadrature to solve two-dimensional incompressible Navier-Stokes equations. Int. J. Numer. Methods Fluids. 15, 791-798 (1992).

[35] Varadan TK, Bhaskar K.: Bending of laminated orthotropic cylindrical shells – An elasticity approach. Comput. Struct. 17, 141-156 (1991).

[36] Cheng ZQ, He LH, Kitipornchai S.: Influence of imperfect interfaces on bending and vibration of laminated composite shells. Int. J. Solids Struct. 37, 2127-2150 (2000).

[37] Heyliger P, Saravanos DA. Exact free vibration analysis of laminated plates with embedded piezoelectric layers. J. Acoust. Soc. Am. 98, 1547–1557 (1995).